Effect of Crystallinity on Magnetic Properties in Manganese-Doped Indium Tin Oxide Films

Saiki Kitagawa[1,2] and Toshihiro Nakamura[1,3]

[1]Graduate School of Human and Environmental Studies, Kyoto University, Kyoto, 606-8501, Japan
[2]Japan Society for the Promotion of Science(JSPS), Chiyoda-ku, Tokyo, 102-0083, Japan
[3]Institute for Liberal Arts and Sciences, Kyoto University, Kyoto, 606-8501, Japan

Mn-doped indium tin oxide (ITO) films were deposited on single crystalline yttria stabilized zirconia (YSZ) substrates with (111) plane orientation and alkali-free glass substrates by rf magnetron sputtering. The epitaxial relationships between the Mn-doped ITO films and YSZ(111) substrates was confirmed by X-ray diffraction measurements. According to the X-ray rocking curve, the epitaxial Mn-doped ITO film on YSZ(111) substrate indicated the high degree of the crystalline alignment. The epitaxial and polycrystalline Mn-doped ITO films exhibited low resistivity and high transparency. Room-temperature ferromagnetism was observed in both the epitaxial and polycrystalline Mn-doped ITO films. The Curie temperature of these films was estimated to be higher than 400 K. The crystallinity difference between the epitaxial and polycrystalline films has little influence on the magnetic properties of the Mn-doped ITO films. The origin of the room-temperature ferromagnetism was discussed on the basis of the correlation between the magnetization and carrier concentration of the Mn-doped ITO films.

***Index Terms*—Diluted magnetic semiconductor, Epitaxial growth, Magnetic film, Transparent conducting film**

I. Introduction

In recent years, dilute magnetic semiconductors (DMSs) have attracted attention as next-generation spintronic materials [1]-[5]. Semiconductors and magnetic materials have played active roles independently in the development of electronic devices. A research field called spintronics was created by the discovery of the giant magnetoresistance effect [6],[7]. To apply DMSs to electronic devices that operate at room temperature, it is necessary that the Curie temperature is above room temperature. Oxide-based DMSs have been reported to exhibit high-temperature ferromagnetism [8]-[12]. Room-temperature ferromagnetism has been observed in some Mn-doped indium tin oxide (ITO) films [13]-[19]. ITO is an n-type wide band gap degenerate semiconductor with high electrical conductivity and high visible transparency, and it is widely used as a transparent conducting film in optoelectronic devices such as flat-panel displays, solar cells, and so on. The coexistence of high-temperature ferromagnetism, high electrical conductivity, and high visible transparency in the Mn-doped ITO films is expected to be a desirable trait for transparent spintronic devices [14],[17]. Magnetron sputtering method for a fabricating of Mn-doped ITO films has good suitability for large area deposition. Integrating Mn-doped ITO films into magneto-optoelectronic devices is simple, since there are several devices using ITO films in the market.

The mechanism for the high-temperature ferromagnetism has not been elucidated in magnetic transparent conducting films such as Mn-doped ITO films with high carrier concentration of 10^{20} - 10^{21} cm^{-3}. The promising candidates of the origin of the ferromagnetism in the Mn-doped ITO films are delocalized charge carrier-mediated interaction [20]-[23] and bound magnetic polaron (BMP) driven interaction via oxygen vacancies [24]-[26]. The crystallinity of thin films is considered to affect the physical properties of the Mn-doped ITO films. Evaluating the effect of crystallinity on magnetic properties of the Mn-doped ITO films is a very important issue to prepare appropriate films for clarifying basic physical properties of magnetic transparent conducting films. In this work, we prepared the epitaxial and polycrystalline Mn-doped ITO films to investigate the crystallinity dependence of magnetic properties of the Mn-doped ITO films. In addition, the electrical and optical properties of the films were also evaluated to discuss the magnetic properties in more detail.

II. Experiment

A. Sample preparation

Mn-doped ITO films were prepared by rf magnetron sputtering on single crystalline yttria stabilized zirconia (YSZ) substrates with (111) plane orientation and alkali-free glass substrates. A sputtering target with an atomic ratio of In : Sn : Mn = 1.75 : 0.2 : 0.05 was used. Before the film deposition, the substrates were cleaned by an ultrasonic cleaner with pure water, ethanol, and acetone for 7 minutes each. After the chamber was evacuated to a low pressure of about 7.0×10^{-4} Pa, pure argon was introduced as a sputtering gas. Before the deposition, the target was pre-sputtered for 60 minutes to obtain a clean target surface. During the sputtering process, the working pressure was kept at 1 Pa. The rf power was 120 W. The substrate temperature was 450 ºC. The deposition time was 30 minutes.

B. Material characterization

The atomic composition of the deposited films was evaluated by the energy dispersive X-ray (EDX) analysis. The crystalline structure of the films was characterized by X-ray diffraion (XRD). Transport properties (resistivity, carrier concentration, and electron mobility) of the films were evaluated by Hall effect measurements using van der Pauw geometry. Optical transmission spectra in the wavelength region of 280 - 780 nm were acquired using a UV-visible spectrophotometer. Magnetic properties of the films were characterized by a superconducting quantum interference device (SQUID) magnetometer.

III. Results and Discussion

To confirm the incorporation of Mn ions in the Mn-doped ITO films, EDX measurements were conducted. The Mn atomic concentration in the Mn-doped ITO films was evaluated to be 1 %. No unintentional elements were present in the Mn-doped ITO films.

To investigate the crystallinity of the Mn-doped ITO films, XRD measurements were carried out. The XRD patterns in 2θ-ω scans for the Mn-doped ITO films deposited on YSZ(111) and alkali-free glass substrates are shown in Figs. 1(a) and (b), respectively. Intense peaks of YSZ(*hhh*) and Mn-doped ITO (*kkk*) diffractions (*h,k* = integer) were observed with no other diffraction peaks in the Mn-doped films grown on YSZ(111) substrates. In contrast, the Mn-doped ITO films deposited on alkali-free glass substrates were identified to be polycrystalline by XRD 2θ-ω scan. No diffraction peak unrelated to the Mn-doped ITO film, which has a cubic bixbyite structure of In_2O_3, and YSZ substrate was observed in the XRD patterns. The lattice constants of Mn-doped ITO films deposited on YSZ(111) and alkali-free glass substrates were confirmed as 1.011 nm and 1.015 nm, respectively. The lattice strain is sufficiently relaxed in the epitaxial Mn-doped ITO film.

Choosing a proper substrate is essential for the epitaxial growth of the Mn-doped ITO film. We used YSZ(111) substrate to grow epitaxial Mn-doped ITO films, because the lattice mismatch between YSZ and In_2O_3 is as small as about 1.3 %. As shown in Fig. 2, the XRD pole figure for the (400) diffraction of the Mn-doped ITO film deposited on YSZ(111) substrate indicated the points of threefold rotational symmetry. As for the film deposited on YSZ(111) substrate, the epitaxial relationship between Mn-doped ITO film and YSZ(111) substrate was confirmed as Mn-doped ITO (111) || YSZ(111). Figure 3 shows X-ray rocking curve for the epitaxial Mn-doped ITO film deposited on YSZ(111) substrate. The full width at half maximum (FWHM) of the (444) peak was as small as 0.29°, indicating the high degree of the crystalline alignment.

The transport properties of the Mn-doped ITO films were investigated by Hall effect measurements using van der Pauw geometry. The resistivity, electron mobility, and carrier concentration of the films are summarized in Table I. The epitaxial Mn-doped ITO films deposited on YSZ(111) substrates show slightly lower resistivity than the polycrystalline films deposited on alkali-free glass substrates. The Mn-doped ITO films deposited on YSZ(111) and alkali-free glass substrates indicated high electron mobility of 37.14 $cm^2V^{-1}s^{-1}$ and 37.83 $cm^2V^{-1}s^{-1}$, respectively. They also exhibited high carrier concentrations of 1.30×10^{21} cm^{-3} and 1.02×10^{21} cm^{-3}, respectively. The crystallinity difference between the epitaxial and polycrystalline films has little influence on the electrical properties of the Mn-doped ITO films. The carrier concentration of the Mn-doped ITO films is higher than that of epitaxial undoped ITO films [27],[28]. Mn ions are possible to have various valence states such as Mn^{2+}, Mn^{3+}, Mn^{4+}, and so on. If Mn^{4+} is replaced at In^{3+} site, one free electron is emitted in the Mn-doped ITO films. This additional free electron may lead to high carrier concentration of the Mn-doped ITO films.

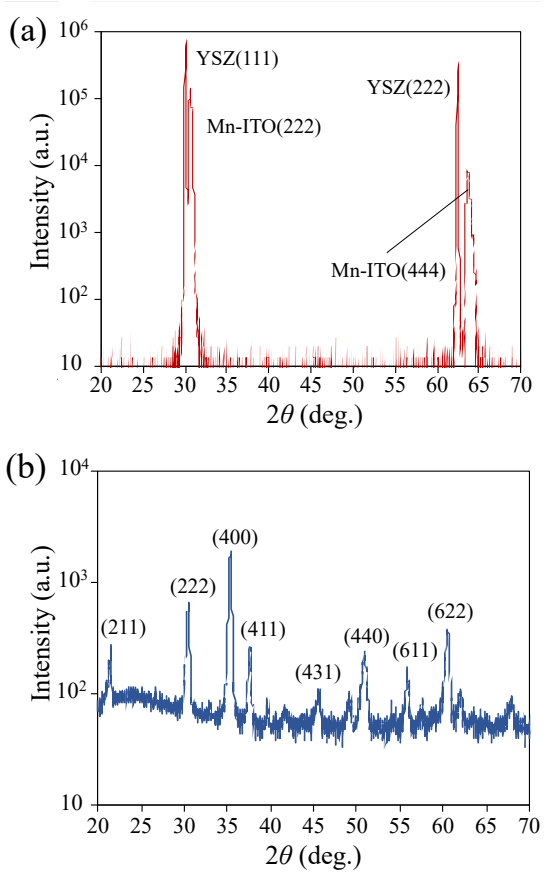

Fig. 1. XRD patterns of the Mn-doped ITO films deposited on (a) YSZ(111) and (b) alkali-free glass substrates.

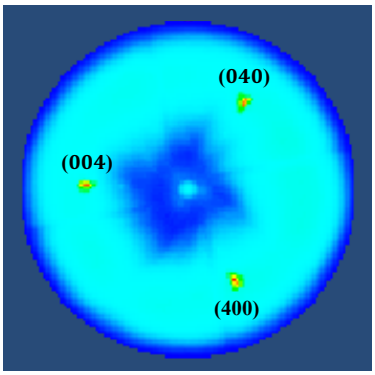

Fig. 2. XRD pole figure for the (400) diffraction of the Mn-doped ITO film deposited on YSZ(111) substrate.

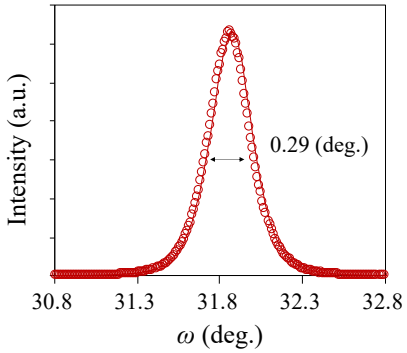

Fig. 3. X-ray rocking curve for the (444) peak of the Mn-dope-ITO film deposited on YSZ(111) substrate.

Table I. Resistivity, electron mobility, and carrier concentration of the Mn-doped ITO films.

Substrate	Resistivity (Ω cm)	Electron mobility ($cm^2V^{-1}s^{-1}$)	Carrier concentration (cm^{-3})
YSZ(111)	1.33×10^{-4}	37.14	1.30×10^{21}
Alkali-free glass	1.61×10^{-4}	37.83	1.02×10^{21}

The optical transmission spectra of the epitaxial and polycrystalline Mn-doped ITO films are shown in Fig. 4. The average transmittance values of the epitaxial and polycrystalline Mn-doped ITO films were about 80 % in the visible region. The deposited Mn-doped ITO films indicated high visible transparency independently of the crystallinity difference of the films.

As shown in Fig. 5, the optical band gap for both the epitaxial and polycrystalline Mn-doped ITO films was estimated to be 3.92 eV by Tauc plots. On the basis of Burstein-Moss shift, the observed optical bandgap for degenerate semiconductors such as ITO significantly depends on the carrier concentration. The difference in the optical bandgap was not observed between epitaxial and polycrystalline Mn-doped ITO films, which shows a good agreement with the experimental data on the carrier concentrations obtained by the Hall measurements (see Table I).

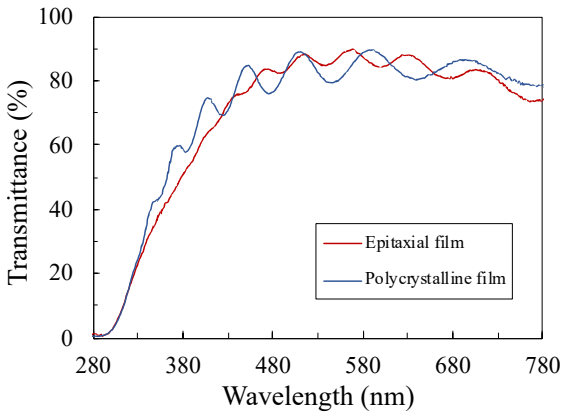

Fig. 4. Comparison of optical transmission spectra between the epitaxial and polycrystalline Mn-doped ITO films.

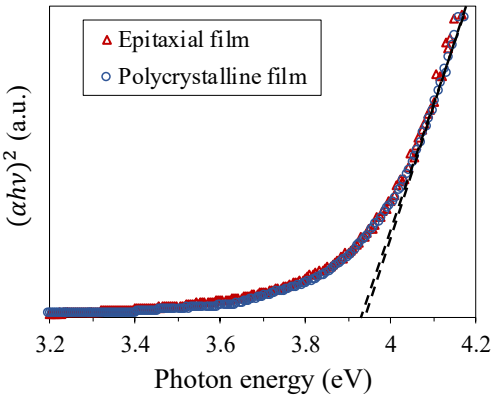

Fig. 5. Tauc plots for the epitaxial and polycrystalline Mn-doped ITO films.

The magnetization versus applied field curves measured at 300 K for the epitaxial and polycrystalline Mn-doped ITO films are shown in Figs. 6(a) and (b), respectively. Both the epitaxial and polycrystalline Mn-doped ITO films exhibit hysteresis loops at 300 K, signifying room temperature ferromagnetism. The saturation magnetization of the epitaxial Mn-doped ITO films is almost the same as that of the polycrystalline Mn-doped ITO films. The coercive force and residual magnetization of the films are summarized in Table II. Although the coercive force and residual magnetization of the epitaxial films are slightly smaller than those of the polycrystalline films, almost no dependence on the crystallinity of the films was found in the behavior of the magnetization of the films. The observed ferromagnetism of the films is not considered to be due to magnetic secondary phase because no extrinsic elements and magnetic impurity phase were detected by EDX and XRD measurements.

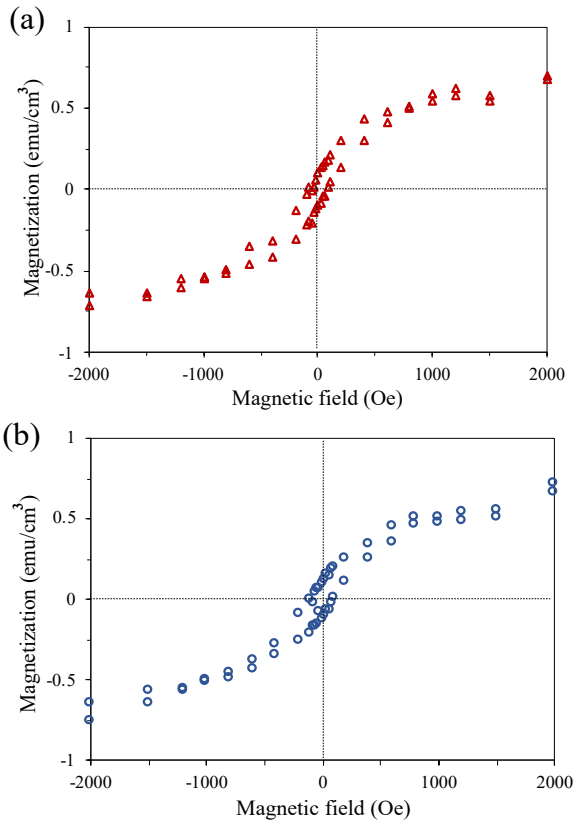

Fig. 6. Magnetization versus applied magnetic field curves measured at 300 K for the (a) epitaxial and (b) polycrystalline Mn-doped ITO films.

Table II. Coercive force and residual magnetization of the Mn-doped ITO films.

Substrate	Coercive force (Oe)	Residual magnetization (emu/cm^3)
YSZ(111)	70	0.10
Alkali-free grass	80	0.11

The Mn-doped ITO films exhibit very high carrier concentrations as compared with dilute magnetic semiconductors other than the Mn-doped ITO films. The delocalized charge carrier-mediated ferromagnetic interaction is one of the most probable candidates of the origin of the ferromagnetism in oxide-based dilute magnetic semiconductors with high carrier concentration [20]-[23]. The delocalized charge carrier-mediated ferromagnetic interactions in the Mn-doped ITO films are considered to occur between the localized Mn spins via the carriers, and significantly depend on the carrier concentration. The carrier concentration of the epitaxial Mn-doped ITO films is almost similar with that of the polycrystalline Mn-doped ITO films as shown in Table I. Therefore, the delocalized charge carrier-mediated ferromagnetic interaction is consistent with the present experimental results that the saturation magnetization of the epitaxial Mn-doped ITO films is almost the same as that of the polycrystalline Mn-doped ITO films.

One of another candidates of the origin of the ferromagnetism in the Mn-doped ITO films is BMP driven interaction via oxygen vacancies [24]-[26]. In this work, the film deposition under the atmosphere of pure Ar gas promoted the generation of oxygen vacancies in the Mn-doped ITO films. The oxygen vacancy constituted BMPs induce ferromagnetic exchange interactions mediated by shallow donor electrons trapped in oxygen vacancies. In this model, the local ferromagnetism is attributed to the F-center (FC) mediated exchange via the electrons trapped in oxygen vacancies [24]-[26]. When the Bohr model is applied to the FC orbit, the FC radius can be expressed as $r_{FC} = \varepsilon_r a_0 (m/m^*)$, where ε_r is the dielectric constant, m is the electron mass, m^* is the effective mass of the donor electrons, and a_0 is the Bohr radius [26]. The Mn ions within the FC radius are exchanged ferromagnetically. For a sufficiently large number of overlapping FC, a long-range ferromagnetic order is established [26]. When the concentration of oxygen vacancies is not sufficient, the long-range ferromagnetic interaction is weak due to a lack of overlapping FC. This picture can explain the weak ferromagnetism observed in the Mn-doped ITO films.

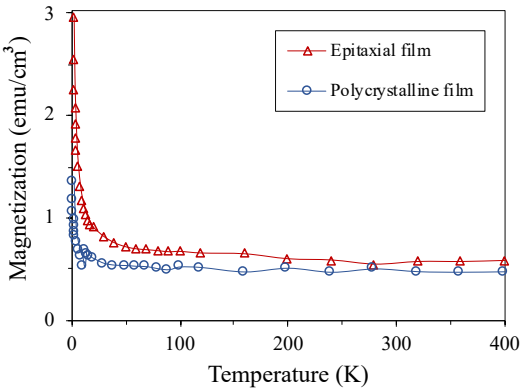

Fig. 7. Temperature dependence of the magnetization for the epitaxial and polycrystalline Mn-doped ITO films under the applied magnetic field of 1000 Oe.

Fig. 7 shows the temperature dependence of the magnetization for the epitaxial and polycrystalline Mn-doped ITO films measured from 2 to 400 K using SQUID. The magnetization data are taken in an applied field of 1000 Oe. The magnetization of the epitaxial Mn-doped ITO films is slightly larger than that of the polycrystalline Mn-doped ITO films in this temperature region. The Curie temperature is estimated to be higher than 400 K, because no reduction to zero was observed at 400 K in the magnetization of the Mn-doped films.

IV. Conclusion

We investigated the crystallinity dependence of the magnetic properties of the Mn-doped ITO films with very high carrier concentration of the order of 10^{21} cm^{-3}. On the basis of the comparison between the epitaxial and polycrystalline Mn-doped ITO films, the electrical, optical, and magnetic properties of the Mn-doped ITO films have little dependence on the crystallinity of the films. The Mn-doped ITO films show high electric conductivity, high visible transparency, and room-temperature ferromagnetism independently of the film crystallinity. The observed room-temperature ferromagnetism in the Mn-doped ITO films is suggested to be not only due to the delocalized charge carrier-mediated ferromagnetic interaction, but also because of the percolation of the oxygen vacancy constituted BMPs. The experiments for more detailed verification of the origin of the high-temperature ferromagnetism is under way.

Acknowledgment

This work was partly supported by JSPS KAKENHI Grant Numbers JP22H02120, JP23KJ1266, and JST SPRING Grant Number JPMJSP2110. The magnetic properties of the films were measured by a Quantum Design MPMS-5S [MPMS-2] system in the Research Center for Low Temperature and Materials Science, Kyoto University. The X-ray diffraction measurements were carried out by a Rigaku SmartLab system in the Nanotechnology Platform of Kyoto University. We thank Prof. Y. Nose group of the Department of Materials Science and Engineering at Kyoto University for their help in Hall effect measurements.

References

[1] H. Ohno, "Making Nonmagnetic Semiconductors Ferromagnetic," *Science,* vol. 281, pp. 951-956, Aug. 1998.

[2] S. A. Worf, D. D. Awschalom, R. A. Buhrman, J. M. Daughton, S. vonMolnar, M. L. Roukes, A. Y. Chtchelkanova, and D. M. Treger, "A Spin-Based Electronics Vision for the Future," *Science*, vol. 294, pp. 1488-1495, Nov. 2001.

[3] T. Dietl and H. Ohno, "Dilute ferromagnetic semiconductors: Physics and spintronic structures," *Rev. Mod. Phys*., vol. 86, pp. 187-251, Mar. 2014.

[4] M. Kobayashi, H. Niwa, Y. Takeda, A. Fujimori, Y. Senba, H. Ohashi, A. Tanaka, S. Ohya, P. N. Hai, M. Tanaka, Y. Harada, and M. Oshima, "Electronic excitations of a magnetic impurity state in the diluted magnetic semiconductor (Ga,Mn)As," *Phys. Rev. Lett.,* Vol. 112, pp. 107203, Mar. 2014.

[5] Y. Takeda, S. Ohya, N. H. Pham, M. Kobayashi, Y. Saitoh, H. Yamagami, M. Tanaka, and A. Fujimori, "Direct observation of the magnetic ordering process in the ferromagnetic semiconductor $Ga_{1-x}Mn_xAs$ via soft x-ray magnetic circular dichroism," *J. Appl. Phys.*, vol. 128, pp. 213902, Oct. 2020.

[6] G. Binasch, P. Grünberg, F. Saurenbach, and W. Zinn, "Enhanced magnetoresistance in layered magnetic structures with antiferromagnetic interlayer exchange," *Phys. Rev. B*, vol. 39, pp. 4828-4830, Mar. 1988.

[7] M. N. Baibich, J. M. Broto, A. Fert, F. Nguyen Van Dau, and F. Petroff, "Giant Magnetroresistance od (001)Fe/(001)Cr Magnetic Superlattices," *Phys. Rev. Lett.*, vol. 61, pp. 2472-2475, Nov. 1988.

[8] Y. Matsumoto, M. Murakami, T. Shono, T. Hasegawa, T. Fukumura, M. Kawasaki, P. Ahmet, T. Chikyow S. Koshihara, and H. Koinuma, "Room-Temperature Ferromagnetism in Transparent Transition Metal-Doped Titanium Dioxide," *Science*, vol. 291, pp. 854-856, Jan. 2001.

[9] K. Ueda, H. Tabata, and T. Kawai, "Magnetic and electric properties of transition-metaldoped ZnO films," *Appl. Phys. Lett.,* vol. 79, pp. 988-990, Aug. 2001.

[10] S. B. Ogale, R. J. Choudhary, J. P. Buban, S. E. Lofland, S. R. Shinde, S. N. Kale, V. N. Kulkarni, J. Higgins, C. Lanci, J. R. Simpson, N. D. Browning, S. Das Sarma, H. D. Drew, R. L. Greene, and T. Venkatesan, "High Temperature Ferromagnetism with a Giant magnetic moment in Transparent Co-doped $SnO_{2-\delta}$," *Phys. Rev. Lett.*, vol. 91, pp. 077205, Aug. 2003.

[11] B. Parveen, M. U. Hassan, Z. Khalid, S. Riaz, and S. Naseem, "Room-temperature ferromagnetism in Ni-doped TiO_2 diluted magnetic semiconductor thin films," *J. Appl. Res. Technol*., vol. 15, pp. 132-139, Mar. 2017.

[12] R. Mohammadigharehbagh, S. Pat, N. Akkurt, and S. Korkmaz, "Studies on the morphological, structural, optical and electrical properties of Fe-doped ZnO magnetic nano crystal thin films," *Physica B*, vol. 609, pp. 412921, Feb. 2021.

[13] J. Philip, N. Theodoropoulou, G. Berera, and J. S. Moodera, "High-temperature ferromagnetism in manganese-doped indium-tin oxide films," *Appl. Phys. Lett.*, vol. 85, pp. 777-779, Jul. 2004.

[14] T. Nakamura, K. Tanabe, K. Tsureishi, and K. Tachibana, "Ferromagnetism in sputtered manganese-doped indium tin oxide films with high conductivity and transparency," *J. Appl. Phys.,* vol. 101, pp. 09H105, Mar. 2007.

[15] X. L. Wang, G. Peleckis, S. X. Dou, R. S. Liu, and J. G. Zhu, "First-Principles investigations of Co- and Fe-doped SnO_2," *J. Appl. Phys.*, vol. 101, pp. 09H104, Mar. 2007.

[16] S. R. Sarath Kumar, P. Malar, T. Osipowicz, S. S. Banerjee, S. Kasiviswanathan, "Ion beam studies on reactive DC sputtered manganese doped indium tin oxide thin films," *Nucl. Instr. and Meth. In Phys. Res. B,* vol. 266, pp. 1421-1424, Dec. 2008.

[17] T. Nakamura, S. Isozaki, K. Tanabe, and K. Tachibana, "Ferromagnetism of manganese-doped indium tin oxide films deposited on polyethylene naphthalate substrates," *J. Appl. Phys.*, vol. 105, pp. 07C511, Feb. 2009.

[18] S. R. Sarath, M. N. Hedhili, H. N. Alshareef, and S. Kasiviswanathan, "Correlation of Mn charge state with electrical resistivity of Mn doped indium tin oxide thin films," *Appl. Phys. Lett.*, vol. 97, pp. 111909, Sep. 2010.

[19] T. Nakamura, "Local structure analysis of magnetic transparent conducting films by X-ray spectroscopy," *J. Phys. D: Appl. Phys.*, vol. 49, pp. 045005, Dec. 2016.

[20] M. J. Calderón and S. D. Sarma, "Theory of carrier mediated ferromagnetism in dilute magnetic oxides," *Ann. Phys.*, vol. 322, pp. 2618-2634, Feb. 2007.

[21] H. Raebiger, S. Lany, and A. Zunger, "Control of Ferromagnetism via Electron Doping in In_2O_3:Cr," *Phys. Rev. Lett.*, vol. 101, pp. 027203, Jul. 2008.

[22] Y. Yamada, K. Ueno, T. Fukumura, H. T. Yuan, H. Shimotani, Y. Iwasa, L. Gu, S. Tsukimoto, Y. Ikuhara, and M. Kawasaki, "Electrically Induced Ferromagnetism at Room Temperature in Cobalt-Doped Titanium Dioxide," *Science*, vol. 332, pp. 1065-1067, May. 2011.

[23] K. Ichihashi, H. Shinya, and H. Raebiger, "Carrier mediated ferromagnetism in Ga_2O_3:Cr," *Appl. Phys. Express*, vol. 13, pp. 021002, Jan. 2020.

[24] P. A. Wolff, R. N. Bhatt, and A. C. Durst, "Polaron-polaron interactions in diluted magnetic semiconductors," *J. Appl. Phys*., vol. 79, pp. 5196-5198, Aug. 1996.

[25] J. M. D. Coey, M. Venkatesan, and C. B. Fitzgerald, "Donor impurity band exchange in dilute ferromagnetic oxides," *Nat. Mater.*, vol. 4, pp. 173-179, Feb. 2005.

[26] X. F. Liu, Y. Sun, and R. H. Yu, "Role of oxygen vacancies in tuning magnetic properties of Co-doped SnO_2 insulating films," *J. Appl. Phys*., vol. 101, pp. 123907, Jun. 2007.

[27] G. Huang, Q. Yu, S. Kou, P. Zhai, and G. Li, "Epitaxial indium tin oxide films deposited on yttrium stabilized zirconia substrate by DC magnetron sputtering," *Physica B*, vol. 601, pp. 412667, Oct. 2021.

[28] M. Kamei, T. Yagami, S. Takaki, and Y. Shigesato, "Heteroepitaxial growth of tin-doped indium oxide films on single crystalline yttria stabilized zirconia substrates," Appl. Phys. Lett., vol. 64, pp. 2721-2714, Aug. 1994.